4500 *Macromolecules* **2009**, *42*, 4500–4510
DOI: 10.1021/ma900094p

Macromolecules
ARTICLE

Electrochemical Behaviors and Anion Recognition of Ferrocene Modified Hyperbranched Polyether

Qiaohua Tan, Li Wang,* Liang Ma, Haojie Yu, Qingquan Liu, and Anguo Xiao

State Key Laboratory of Chemical Engineering, Department of Chemical and Biological Engineering, Zhejiang University, Hangzhou 310027, PR China

Received January 16, 2009; Revised Manuscript Received May 21, 2009

ABSTRACT: A series of ferrocene modified hyperbranched polyethers **HBPO-Fc** with different ferrocene content were obtained by cation ring-opening polymerization followed by esterification. Electrochemical behaviors of **HBPO-Fc** were investigated by cyclic voltammetry (CV) and the influence of ferrocene content of **HBPO-Fc**, scan rate, solvent and electrolyte concentration on the electrochemical behaviors of **HBPO-Fc** were discussed, and the dynamic parameters in electrode processes were calculated. Anion recognition of **HBPO-Fc** was studied by CV and UV−vis. The binding capacities of **HBPO-Fc** to different anions were compared, and the binding capacities of **HBPO-Fc** with different ferrocene content were also discussed. Finally, binding models of **HBPO-Fc** to anions were proposed.

1. Introduction

Due to the rapid development of biology, anion recognition by supermolecular interaction is becoming a hot area of study,[1,2] because anions play crucial part in biology. One of the most important topics in anion recognition is to design and synthesize artificial anion receptors with high sensitivity and selectivity.[3] Dendrimers as anion receptors have now attracted many chemists' interest;[4−7] one reason is that the 3-D structures of dendrimers resemble the morphology of viruses, cancer cells and other biology molecules,[4] and the investigation of dendrimers in anion recognition will help to uncover some biology processes. The other reason is because of its "dendritic effect", which means that, compared with the small molecule, the anion recognition ability of dendrimer anion receptors increased with the increasing generations.[4−7] Astruc[4−7] has done much work on the anion recognition of dendrmers and has been able to explain the "dendritic effect". With the increase of the generation of dendrimers, the surface hole of dendrimers decreased because the dendritic branches become closer to one anther, and the smaller hole will be certainly more compatible with the anions which have small sizes. In general, the dendritic effect is the result of size compatibility of the cavities in the surface of dendrimers with anions. Though the dendrimers have apparent advantages in anion recognition, the difficulties in preparing dendrimers with perfect molecular structures have greatly limited the use of them. However, hyperbranched polymers which do not have perfect molecular structures like dendrimers, keep some properties of dendrimers such as having cavities in the surface, having many functional groups outside, ease of film forming, and good solubility, to name a few.[8] These favorable properties just mentioned have allowed hyperbranched polymers to act as effective anion receptors. Most importantly, hyperbranched polymers are much easier to prepare than dendrimers.[8] Up to now, various hyperbranched polymers with high thermal stability and great strong optical properties have been reported by Benzhong's group.[9] However, hyperbranched polymers were seldom reported in anion recognition.[10]

*Corresponding author. Telephone: +86-571-8795-3200. Fax: +86-571-8795-1612. E-mail: opl_wl@dial.zju.edu.cn.

Electrochemical methods such as cyclic voltammetry (CV) are some of the most important methods used in anion recognition because of their effective detection, ease of operation, and low cost. Many anion receptors were designed based on the electrochemical method, such as ferrocenyl anion receptors. As we know, the electrochemical behaviors are influenced by many factors, such as scan rate, electrolyte concentration and redox center concentration.[11−14] However, in the anion recognition of ferrocenyl anion receptors by electrochemical method reported, no one has considered these factors.

In this paper, we synthesized a new kind of ferrocene modified hyperbranched polyether with different ferrocenyl content through cationic ring-opening polymerization and then followed esterification, and investigated the electrochemical behaviors of them through CV, discussed the influence of scan rate, electrolyte concentration and redox concentration. The anion recognition of this kind of hyperbranched polyether was also studied.

2. Experimental Section

2.1. Reagents. All the reagents in use are from commercial markets. Before use, ferrocene carbonate acid (AR) was dried in a vacuum, and solvents such as CH_2Cl_2 (AR), $CHCl_3$ (AR), *N*, N-dimethylformamide (DMF, AR), and dimethyl sulfoxide (DMSO, AR) were distilled twice in presence of molecular sieve. Other solid reagents such as $LiClO_4$ (AR) and Bu_4NBF_4 (95%), $Bu_4NH_2PO_4$, Bu_4NHSO_4, and Bu_4NBr were directly used.

2.2. Instruments. The CV measurements of solution were carried out with a CHI-600A Electrochemical Analyzer (CH Instruments, Inc., Austin, TX) in an undivided three electrode cell. The working electrode was a Teflon-shrouded glassy carbon disk electrode (Φ = 3 mm, geometric area = 0.071 cm^2), which was polished to a mirror finish with 0.05-μm Al_2O_3 paste on felt, cleaned by ultrasonication successively in 0.1 M NaOH, 1:1 HNO_3, anhydrous ethyl alcohol, and double distilled water, and then dried and used for electrochemical measurements. Pt wire was used as the counter electrode, Ag wire was used as the reference electrode in organic solvents, and a Ag/AgCl (3 M KCl) electrode was used as the reference electrode in aqueous solution.The solution ohmic potential (*iR*) drop of the investigated solution was measured and autocompensated with CHI-600A electrochemical analyzer. Every CV experiment

 Published on Web 06/09/2009

was repeated three times in order to obtain the reproducible result. IR spectra of the polymers were obtained using a Nicolet 5700 FT-IR Instrument. ^{1}H NMR spectra were recorded on an Advanx-500 NMR Instrument with $CDCl_3$ as solvent. UV−vis spectra were carried out by an HP 8453 UV−vis instrument. Gel permeation chromatography (GPC) analysis was carried out with a Waters 1515 GPC instrument and monitored by thermal conductivity detector. The mobile phase was THF eluent at a flow rate of 1.0 mL/ min, and samples were calibrated against polystyrene at 30 °C.

2.3. Hyperbranched Polyether Film-Coated Electrodes. Hyperbranched polyether film-coated electrodes were prepared by covering the glassy carbon disk electrodes with a solution of hyperbranched polyether in THF (3.9 g/L) and then allowing the solvent to evaporate at room temperature.

2.4. Synthesis of 3-Ethyl-3-(hydroxymethyl)oxetane (EOM). 3-Ethyl-3-(hydroxymethyl)oxetane (**EOM**) was prepared by a modified procedure described in the literature.[15] A mixture of trimethyloxypropane (**1**, 26.8 g, 0.2 mol), diethyl carbonate (23.6 g, 0.2 mol), KOH (0.1 g, 1.8 mmol) in 2 mL of absolute ethyl alcohol was refluxed in oil bath at 110 °C for 1 h, then distilled for 1 h. The temperature of the oil bath was increased to 140 °C and distillation was continued for 1 h. With an oil bath temperature of 185 °C, 19.5 g of product was collected under vacuum, with a yield of 84.0%.

2.5. Synthesis of Poly(3-ethyl-3-(hydroxymethyl)oxetane) (HBPO). Poly(3-ethyl-3-(hydroxymethyl)ox etane) was prepared by procedure described in the literature.[16] In the ice bath control of 0 °C, $BF_3 \cdot OEt_2$ (0.05 mol BF_3) was added to the three-necked flask containing 100 mL of CH_2Cl_2, and then 11.6 g (0.1 mol) of monomer 3-ethyl-3-(hydroxymethyl)oxetane (EOM) was added quickly under the protection of Ar. After 24 h of polymerization, the product was obtained by precipitating the mixture in water. The product was collected and dried in a vacuum to obtain 10.0 g of pure product. (Yield = 86.0%.)

2.6. Synthesis of ferrocene modified poly(3-ethyl-3-(hydroxymethyl) oxetane) (HBPO-Fc). Ferrocene modified poly (3-ethyl-3-(hydroxymethyl)oxetane) was prepared by a modified procedure described in the literature.[17] An 0.50 g (0.34 mmol, −OH 1.0 mmol) sample of poly(3-ethyl-3-(hydroxymethyl) oxetane) (HBPO) was put into the 50 mL three-necked flask, and then 20 mL of anhydrous CH_2Cl_2 and excess NEt_3 was added. After HBPO was solved, 20 mL anhydrous CH_2Cl_2 containing 0.13 g (0.5 mmol) ferrocenyl chloride was added dropwise. The reaction was stirred at room temperature for 20 h and then filtered. Filtrate was washed with $NaHCO_3$ aqueous solution (0.3 wt %) three times, and then dried by $MgSO_4$. We removed the solvent in vacuum; the orange solid product **HBPO-Fc1** was obtained. Under the same operating conditions with **HBPO-Fc1,** the yellow solid product **HBPO-Fc2** with more ferrocenyl content was obtained in which the amount of ferrocenyl chloride was 0.32 g (1.3 mmol).

3. Results and Discussion

3.1. Characterization of EOM, HBPO, and HBPO-Fc. The synthesis routes of monomer EOM, hyperbranched polyether HBPO, and ferrocenyl modified hyperbranched polyether **HBPO-Fc1** and **HBPO-Fc2** were shown in Scheme 1.

^{1}H NMR of EOM, HBPO, and HBPO-Fc were shown in Figure 1, and the ^{1}H NMR spectrum of EOM showed peaks with the following shift: 0.80−0.83 (−CH_2CH_3), 1.61−1.66 (−CH_2CH_3), 3.62 (−CH_2OH), 3.66 (−CH_2O*H*), 4.31−4.32 and 4.38−4.39 (−CH_2O), which correspond to the structure of expected product. The ^{1}H NMR spectrum of HBPO showed peaks with the following shift: 0.82−0.85 (−CH_3), 1.16−1.29 (−CH_2CH_3), 2.85−3.10 (−CH_2OH), 3.35−3.68 (−OCH_2−), which correspond to the structure of expected product. The ^{1}H NMR spectrum of **HBPO-Fc** showed peaks with the following shift: 0.82−0.85 (−CH_3), 1.16−1.29 (−CH_2CH_3), 3.35−3.68 (−OCH_2−, −CH_2−OH), 4.21 (−CH_2OCO−), 4.3−4.9 (Fc-*H*), which correspond to the structure of expected product. Comparing the ^{1}H NMR spectrum of **HBPO-Fc** with HBPO, we found that in the proton shift of −CH_2− connected with −OH at 2.85−3.10 in ^{1}H NMR spectrum of HBPO disappeared, and a new shift at 4.21 appeared which attributed to −CH_2− connected to ester group. The total disappearance of the proton shift of −CH_2− connected with −OH was not expected, but this may be because that the position of this peak was close to the broad shoulder peak and the intensity decrease made it hard to distinguish from the broad shoulder peak.

The UV−vis spectra of two ferrocenyl modified hyperbranched polyethers, **HBPO-Fc1** and **HBPO-Fc2**, were shown in Figure 2. It can be found that there were three character peaks in UV−vis of **HBPO-Fc1** and **HBPO-Fc2**, which is at λ_{max} = 266, 321, and 449 nm. The peak at 266 nm was the character peak of the ester group, and the peaks at 321 and 449 nm were due to the ferrocene group.

The GPC data of HBPO, **HBPO-Fc1**, and **HBPO-Fc2** were shown in Table 1. It was found that the introduction of ferrocene group to the molecule of HBPO led to an increase in the molecule weight, but the polydistribution index (PDI) showed little change. From the molecular weight of HBPO, **HBPO-Fc1**, and **HBPO-Fc2**, the average number of ferrocene groups per **HBPO-Fc** can be calculated. We find that the ferrocene content of **HBPO-Fc2** was larger than that of **HBPO-Fc1**, which was in accordance with the H NMR spectra and UV−vis spectra above.

It was also found that in the same mass concentration, the two ferrocenyl modified hyperbranched polyethers **HBPO-Fc1** and **HBPO-Fc2** showed different peak intensities. The larger peak intensity of **HBPO-Fc2** indicated a larger content of ferrocene group and ester group.

3.2. Electrochemical Behaviors of HBPO-Fc. *3.2.1. Influence of Ferrocene Content on Electrochemical Behaviors of **HBPO-Fc**.* Electrochemical behaviors of **HBPO-Fc1** and **HBPO-Fc2** in CH_2Cl_2 were investigated. CV curves of **HBPO-Fc1** and **HBPO-Fc2** were shown in Figure 3. It was found that CV curves of **HBPO-Fc1** and **HBPO-Fc2** all showed one pair of redox peaks, which indicated that both **HBPO-Fc1** and **HBPO-Fc2** involved almost the uniform chemical environment of the ferrocene group. However, the redox behaviors of **HBPO-Fc1** and **HBPO-Fc2** were broad because of the broad PDI of **HBPO-Fc1** and **HBPO-Fc2** . This made the chemical environments of the ferrocene group have a slight difference. The electrochemical data of **HBPO-Fc1** and **HBPO-Fc2** were listed in Table 2. It was found that the peak-to-peak separation ΔE_p was very large, indicating the CV curves were irreversible.[18] Though solutions of **HBPO-Fc1** and **HBPO-Fc2** had the same concentration of ferrocene groups, the peak current of **HBPO-Fc2** was much smaller than that of **HBPO-Fc1**, which may be explained by the fact that **HBPO-Fc2** has more ferrocene groups in the molecule, when the total concentrations of ferrocene group in the solutions were the same, concentration of **HBPO-Fc2** molecule was thus much lower, so the mass transfer and the electron exchange efficiency may be lower leading to the relatively smaller peak currents.

*3.2.2. Influence of Scan Rate on Electrochemical Behaviors of **HBPO-Fc**.* Electrochemical behaviors of **HBPO-Fc** with different scan rates in CH_2Cl_2 were investigated, and CV curves of **HBPO-Fc1** and **HBPO-Fc2** were shown in Figure 4. It was found that with the increase of scan rate, peak currents i_p increased, and over a broad scan rate range, i_p were proportional to the square root of the scan rate ($v^{1/2}$).

Scheme 1. Synthesis Route of Monomer EOM, Hyperbranched Polymer HBPO, and Ferrocenyl Modified Hyperbranched Polymer HBPO-Fc

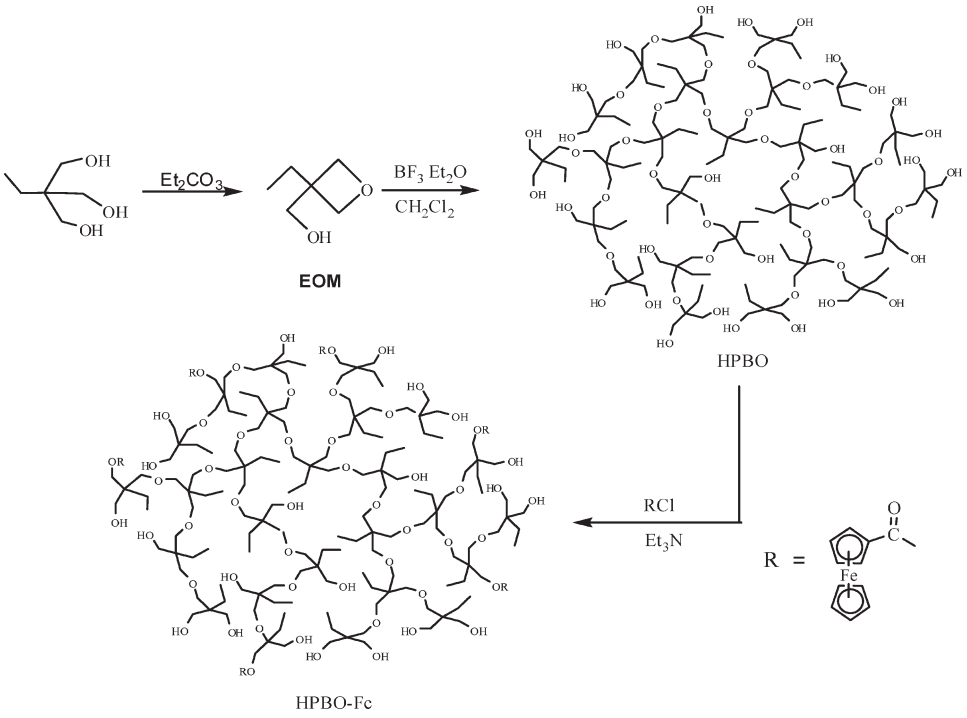

(The results of the linear correlation between i_p and $v^{1/2}$ are listed in Table S1). This indicated that the charge transport obeys Fick's law and the electrode processes were diffusion controlled.[18] And with the increase of scan rate, the reduction peak shifted to the low potential, and the oxidation shifted to the high potential, thus peak-to-peak potential ΔE_p increased, but $E_p^{1/2}$ almost stayed the same. The relationship between the peak potential ($E_p - E^{0'}$) and the logarithm of potential scan rate ln$v$ of **HBPO-Fc1** and **HBPO-Fc2** were shown in Figure 5. ($E_p - E^{0'}$) shifted with ln$v$, but was nonlinear. At slow scan rates, the variability of peak potential with potential scan rate changed slightly. Along with the increase of potential scan rate, the variability of peak potential increased. According to the theory of CV,[18] the peak potential E_p is independent of scan rate and $\Delta E_p < 60$ mV in a reversible electrode process. Also, in a totally irreversible process, there is a linear relationship between the peak potential and the logarithm of the scan rate and $\Delta E_p > 60$ mV. The experimental results indicated that the electrochemical processes of **HBPO-Fc1** and **HBPO-Fc2** in CH_2Cl_2 were neither totally irreversible nor simply reversible. It was obvious that the electron-transport rate in the process was slow. Although the electrode processes were diffusion controlled, the rate of the electrode reaction were rather slow. Thus the larger the potential scan rate was, the possibility that the electrode reaction reached completion in time is less.Therefore, the CV process was controlled by both mass diffusion and electrode reaction.

According to the CV theories,[18] for an irreversible process, there are relationships between peak current, peak potential, and potential scan rate as follows:

$$i_p = 0.4985nFAC_0^*\left(\frac{F}{RT}\right)^{1/2}(\alpha n_\alpha)^{1/2}D_0{}^{1/2}v^{1/2} \quad (1)$$

$$i_p = 0.227nFAC_0^*k^0\exp\left[-\frac{\alpha n_\alpha F}{RT}(E_p - E^{0'})\right] \quad (2)$$

Here n, A, D_0, αn_α, k^0 are the electrochemical stoichiometry, surface area of the electrode (cm^2), diffusion coefficient of electroactive species (cm^2 /s), concentration of electroactive species in solution(mol/cm^3), surface transfer coefficient, and standard rate constant (cm /s), respectively. From Table 3, eq 1, and eq 2, αn_α, D_0, and k^0 of **HBPO-Fc1** and **HBPO-Fc2** in CH_2Cl_2 can be calculated and were also listed in Table 3. Generally, αn_α represents electrode surface electron exchange efficiency, reflects the reversibility of electrode process, and influences the peak potentials and the symmetry of the curves. With the decrease of αn_α, the peak-to-peak potential ΔE_p increases, and the reversibility decreases. From Table 3, we found that αn_α values of **HBPO-Fc1** and **HBPO-Fc2** were small, which indicated the low electrode surface electron exchange efficiency and was reflected by the low reversibility. Also, αn_α of **HBPO-Fc2** was relatively lower than that of **HBPO-Fc1**, which was in agreement with the reversibility of **HBPO-Fc1** and **HBPO-Fc2**. Comparing the reduction and oxidation states of **HBPO-Fc1** and **HBPO-Fc2**, αn_α of reduction state was higher than the oxidation state, which may be the result of the instability of the oxidized ferrocenium. For the diffusion coefficient D_{app}, D_{app} of **HBPO-Fc1** was also larger than that of **HBPO-Fc2**.

3.2.3. Influence of Solvents on Electrochemical Behaviors of HBPO-Fc. Electrochemical behaviors of **HBPO-Fc1** in different organic solvents such as CH_2Cl_2, $CHCl_3$, DMF, and DMSO were investigated (Figure 6). We found that solvents had much influence on the electrochemical behaviors of **HBPO-Fc1**, and in different solvents the CV curves of **HBPO-Fc1** showed apparent difference. The peak shape, peak potential and the peak current all differed. In CH_2Cl_2 and $CHCl_3$, the CV curves of **HBPO-Fc1** had apparent and relative symmetric redox peaks, but in polar solvents such as DMF and DMSO, the CV peaks were badly distorted. These may be the results of aggregating of two near hydrophobic ferrocene moietes appended due to the hydrophobic interaction.[19,20] We investigated the electrode kinetics of **HBPO-Fc1** in CH_2Cl_2 and $CHCl_3$, and we calculated the kinetic

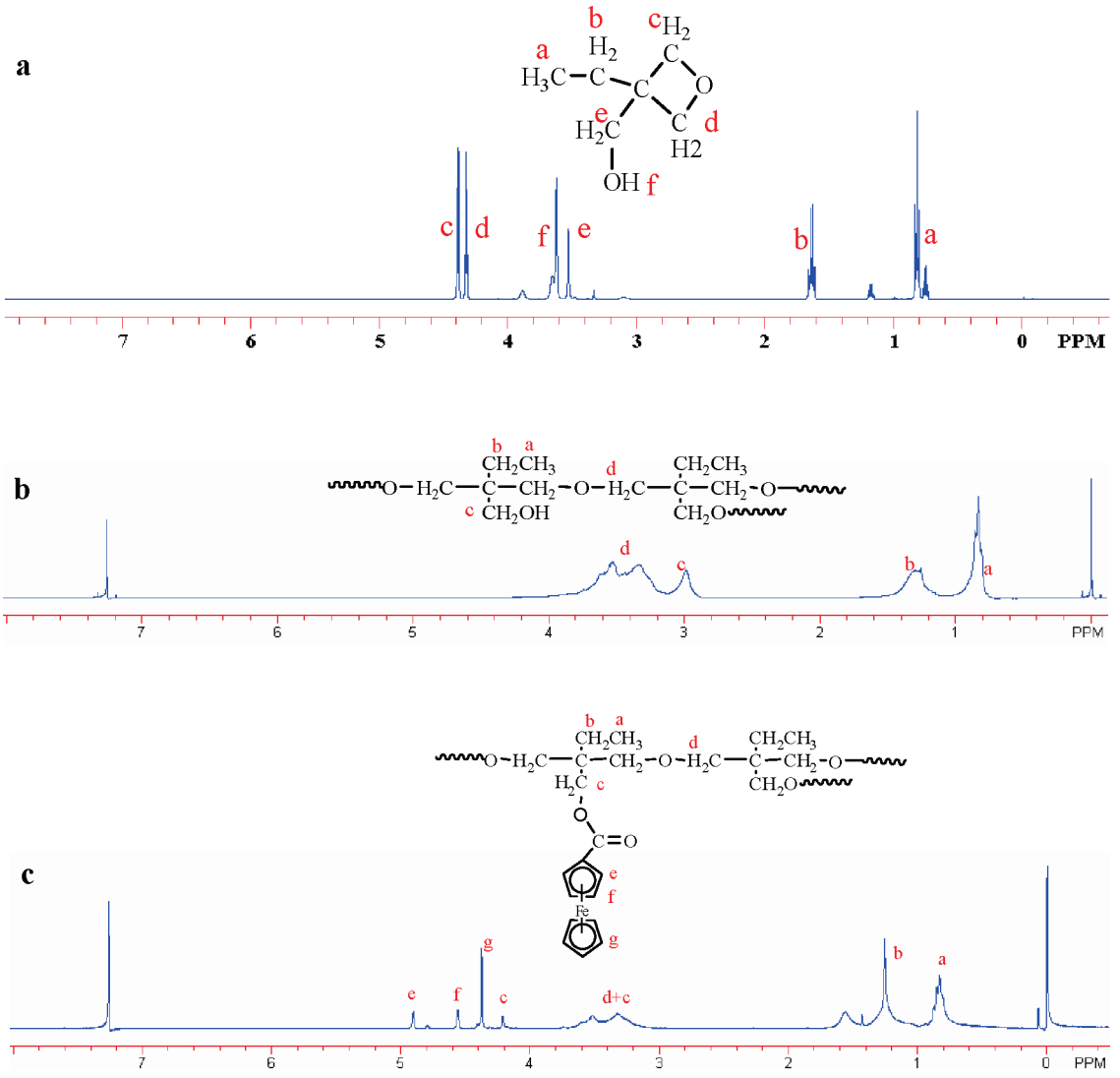

Figure 1. ^{1}H NMR spectra of EOM (a), HBPO (b), and **HBPO-Fc** (c).

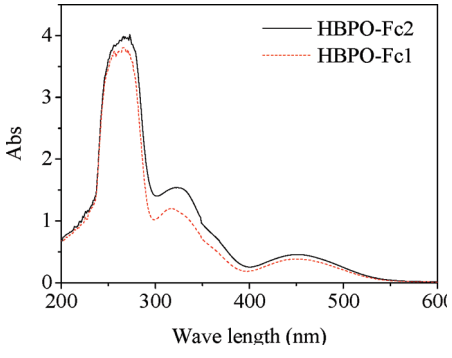

Figure 2. UV−vis spectra of **HBPO-Fc1** and **HBPO-Fc2** in $CHCl_3$ with a mass concentration of 8.3 g/L.

Table 1. GPC Data of Hyperbranched Polymer HBPO, HBPO-Fc1 and HBPO-Fc2

compound	M_n	M_w	PDI	n_{Fe}
HBPO	1456	2140	1.47	
HBPO-Fc1	1655	2384	1.44	1
HBPO-Fc2	1855	2756	1.49	2

parameters through formulas 1 and 2, and the kinetic parameters are listed in Table 3. It was found that αn_α of **HBPO-Fc1**

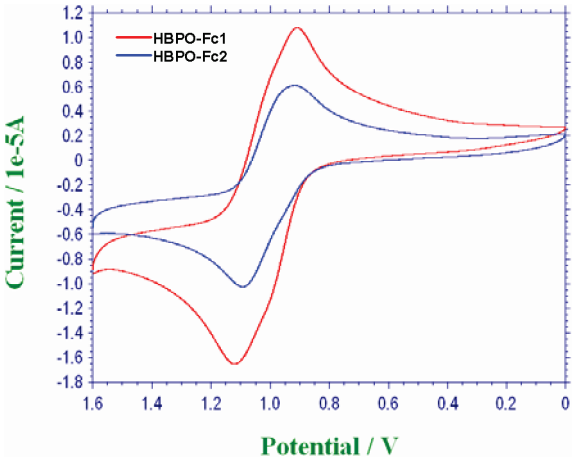

Figure 3. CV curves of **HBPO-Fc1** and **HBPO-Fc2** in CH_2Cl_2. Electrolyte: 0.1 M $[Bu_4N]BF_4$. [Fe]: 0.5 mM. Scan rate: 0.1 V/s.

in $CHCl_3$ was much smaller than that in CH_2Cl_2, indicating that the electron exchange efficiency was very low, which was reflected by the much larger peak-to-peak potential separation ΔE_p and the much smaller reversibility (the electrochemical data were listed in Table 2). However, the standard rate

Table 2. Electrochemical Data of HBPO-Fc

solvent	$C_{Electrolyte}$ (M)	sample	E_{pc} (V)	E_{pa} (V)	$E_p^{1/2}$ (V)	ΔE_p (V)	i_{pc} (10^6A)	i_{pa} (10^{-6}A)	i_{pa}/i_{pc}
CH_2Cl_2	0.1	**HBPO-Fc1**	0.909	1.120	1.015	0.211	14.80	−15.83	1.07
CH_2Cl_2	0.1	**HBPO-Fc2**	0.900	1.069	0.985	0.169	9.483	−10.99	1.16
$CHCl_3$	0.1	**HBPO-Fc1**	0.733	1.109	0.921	0.376	9.933	−9.867	0.993
CH_2Cl_2	0.075	**HBPO-Fc1**	0.870	1.088	0.979	0.218	15.93	−16.58	1.04
CH_2Cl_2	0.05	**HBPO-Fc1**	0.862	1.109	0.986	0.247	14.94	−15.47	1.04
CH_2Cl_2	0.025	**HBPO-Fc1**	0.838	1.174	1.006	0.336	15.49	−15.94	1.03

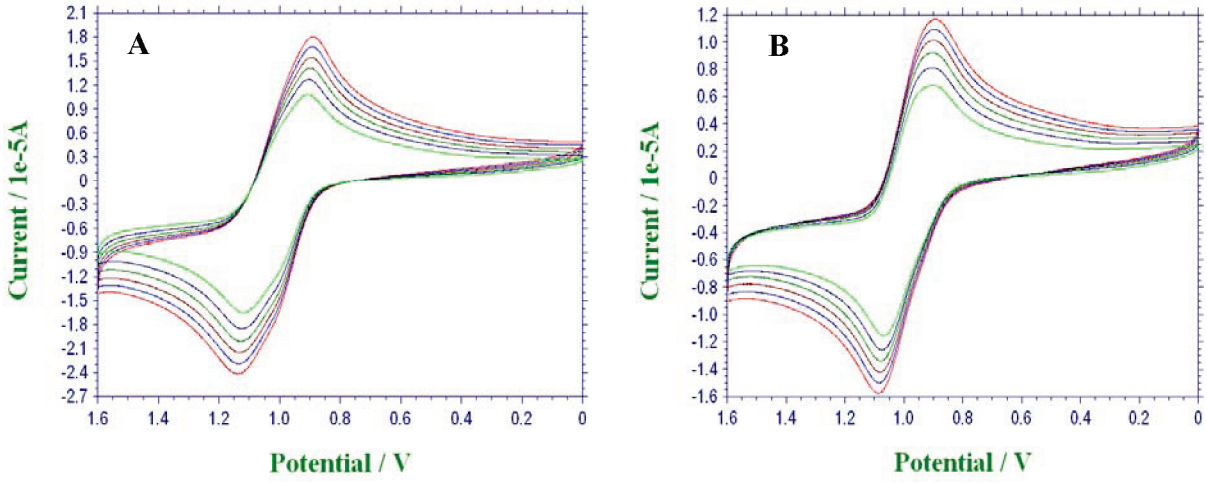

Figure 4. CV curves of **HBPO-Fc1** (A) and **HBPO-Fc2** (B) with different scan rates in CH_2Cl_2. Electrolyte: 0.1 M $[Bu_4N]BF_4$. [Fe]: 0.5 mM. From inner to outer, the scan rates are 0.1, 0.14, 0.18, 0.22, 0.26, and 0.30 V/s.

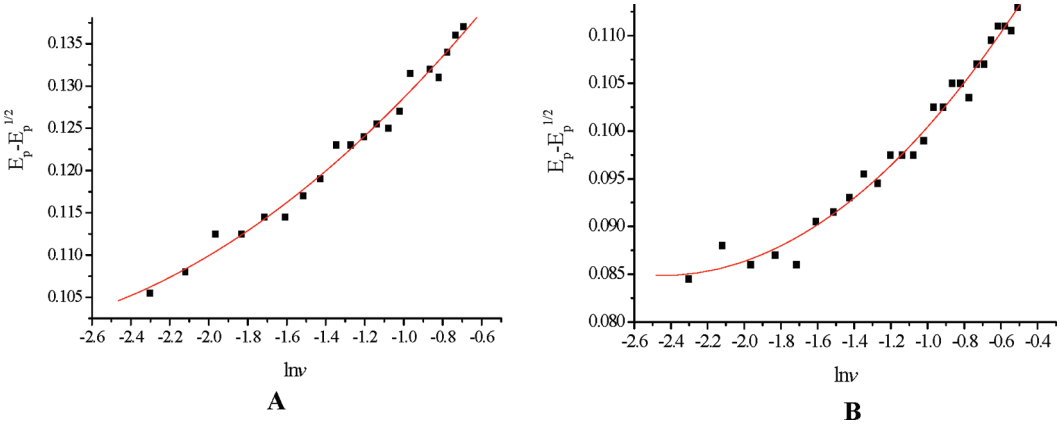

Figure 5. Relationships of $E - E_p^{1/2}$ and ln v of **HBPO-Fc1** (A) and **HBPO-Fc2** (B).

Table 3. Kinetic Parameters of Electrode Processes for HBPO-Fc1 and HBPO-Fc2

solvent	electrolyte concentration (M)	sample	peak type	αn_α	k^0 (cm/s)	D_{app} (10^6 cm^2/s)
CH_2Cl_2	0.1	**HBPO-Fc1**	reduction	0.470	7.24	16.948
			oxidation	0.418	9.46	15.833
		HBPO-Fc2	reduction	0.397	9.49	5.100
			oxidation	0.346	12.33	4.945
$CHCl_3$	0.1	**HBPO-Fc1**	reduction	0.124	13.04	24.87
			oxidation	0.106	15.21	22.06
	0.075	**HBPO-Fc1**	reduction	0.428	8.63	22.39
			oxidation	0.371	11.33	19.32
CH_2Cl_2	0.05	**HBPO-Fc1**	reduction	0.335	9.74	19.98
			oxidation	0.279	12.68	15.94
	0.025	**HBPO-Fc1**	reduction	0.213	12.44	39.58
			oxidation	0.167	17.34	30.77

constant k_0 and diffusion coefficient D_{app} of **HBPO-Fc1** in $CHCl_3$ were much larger than those in CH_2Cl_2, indicating that the electron exchange rate and the diffusion in $CHCl_3$ were larger.

*3.2.4. Influence of Electrolyte Concentration on Electrochemical Behaviors of **HBPO-Fc**.* Electrochemical behaviors of **HBPO-Fc1** in CH_2Cl_2 with different electrolyte concentration were investigated. Figure 7A showed the CV curves

of **HBPO-Fc1** with different electrolyte concentration. It was found that with different electrolyte concentration, the CV curves of **HBPO-Fc1** showed much difference including the peak potential, peak currents. The electrochemical data of **HBPO-Fc1** with different electrolyte concentration were listed in Table 3. It was found that with the increase of electrolyte concentration, the peak-to-peak potential separation ΔE_p gradually decreased (Table 2). And when in low electrolyte concentration, the peak-to-peak potential separation ΔE_p changed dramatically with the change of electrolyte concentration. However, when electrolyte concentration went higher, ΔE_p changed not as dramatically as in the low electrolyte concentration. This may be explained by the fact that when in low electrolyte concentration, the electrode process was mainly controlled by mass diffusion, and the influence of electrolyte concentration was dramatic. When electrolyte concentration increased to some degree, the electrode process changed to be mainly controlled by electrode reaction; thus, the influence of electrolyte concentration was not so apparent. The electrode dynamics of **HBPO-Fc1** with different electrolyte concentration were also studied, and the dynamic parameters were calculated (listed in Table 3). We found that the change tendency of surface exchange efficiency αn_α was in agreement with peak-to-peak potential separation ΔE_p, thus surface exchange efficiency αn_α increased with the increase of electrolyte concentration (Figure 7B). And when in low electrolyte concentration, αn_α changed dramatically; when electrolyte concentration increased, the change rate of αn_α decreased.

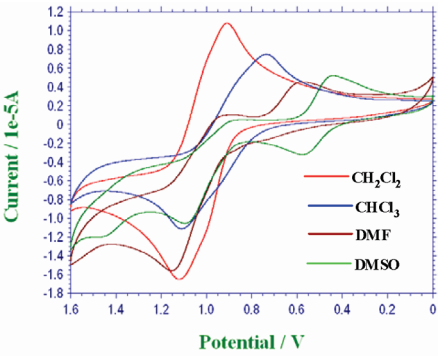

Figure 6. CV curves of **HBPO-Fc1** in varous solvents. Electrolyte: 0.1 M $[Bu_4N]BF_4$; .[Fe]: 0.5 mM. Scan rate: 0.1 V/s.

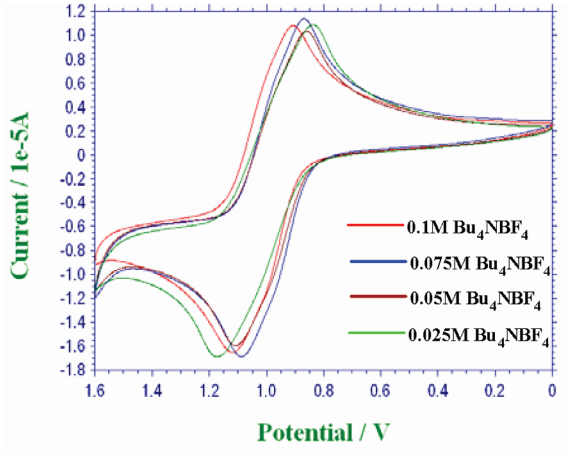

A

*3.2.5. Electrochemical Behaviors of **HBPO-Fc** Film.* Hyperbranched polymers form films easily, thus we also investigated the electrochemical behaviors of **HBPO-Fc** when forming film on the surface of the electrodes. Figure 8 showed the CV curves of **HBPO-Fc1** and **HBPO-Fc2** films in water. It was found that with successive scan, the CV curves of **HBPO-Fc1** and **HBPO-Fc2** films were not stable and the peak currents kept weakening, which may be the results of the instability of oxidized ferrocenium and the destruction of the film.[11] Compared with the CV curves of small ferrocenyl compound film we reported before, the CV curves of **HBPO-Fc1** did not show the process of peak current increase, which may be explained by that the hyperbranched polymer film was much looser, which made the swelling of film and the permeation of supporting electrolyte much easier, and thus the time for this process was too short to be shown in CV curves. From Figure 8, CV shapes of **HBPO-Fc1** and **HBPO-Fc2** were not favorable and the peak currents were small, which may be the result of the poor film-swelling capacity of water. For the hydrophobic **HBPO-Fc1** and **HBPO-Fc2** films, the organic solvents may have much larger film-swelling capacity, thus the electrochemical behaviors of **HBPO-Fc1** and **HBPO-Fc2** films in organic solvents were also investigated.

Figure 9 showed the CV curves of **HBPO-Fc1** and **HBPO-Fc2** films in water, methanol, ethanol, 2-propanol, and *n*-butanol. It was found that the peak currents i_p increased in the order water < methanol < ethanol < *n*-butanol < 2-propanol, which was the order of hydrophobic film-swelling capacity and proved that the better the film-swelling capacity, the larger the peak currents were. The quantity of electricity of the CV peaks of **HBPO-Fc1** and **HBPO-Fc2** films Q_C in different solvents were listed in Table 4. From Q_C, it was directly found how many redox centers were involved in the electrode reaction. In water, methanol and ethanol, Q_C of **HBPO-Fc1** and **HBPO-Fc2** were much small, and in 2-propanol and *n*-butanol, Q_C of **HBPO-Fc1** and **HBPO-Fc2** were larger. Relatively, Q_C of **HBPO-Fc2** was larger than that of **HBPO-Fc1**, and this distinction was especially dramatic in water, methanol, and ethanol. These may be the results of the larger redox center density of **HBPO-Fc2**.

3.3. Anion Recognition Investigation of HBPO-Fc. *3.3.1. Anion Recognition Investigation of **HBPO-Fc** by CV.* Anion recognition of **HBPO-Fc1** and **HBPO-Fc2** were investigated. Figure 10 showed the CV responses of **HBPO-Fc1**

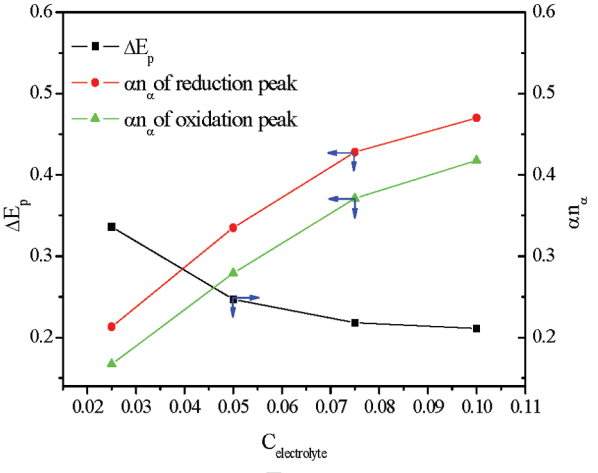

B

Figure 7. (A) CV curves of **HBPO-Fc1** with different electrolyte concentrations in CH_2Cl_2; [Fe]: 0.5 mM; scan rate: 0.1 V/s. (B) Changes of peak-to-peak difference ΔE_p of CV curves and surface transfer coefficient αn_α of **HBPO-Fc1** with the change of electrolyte concentration.

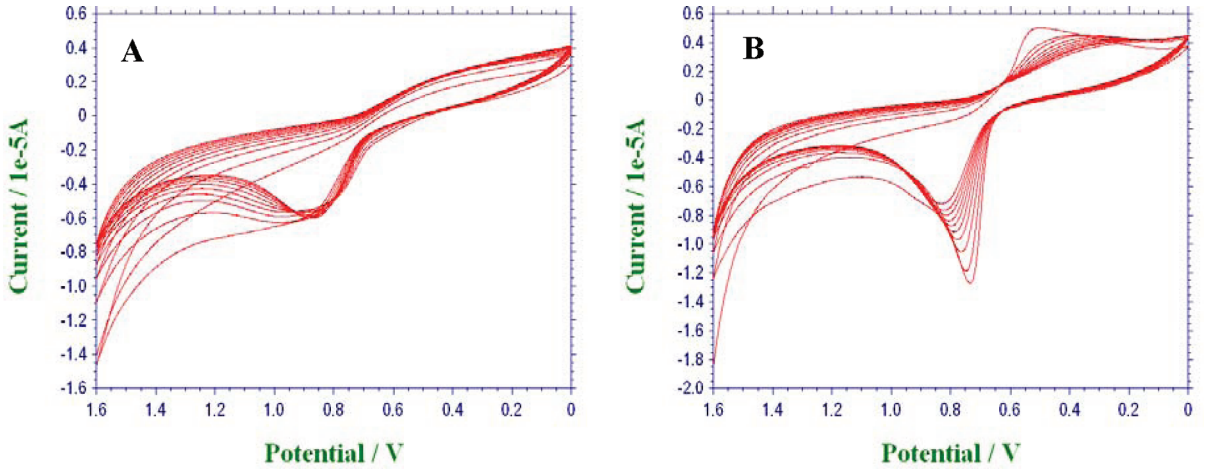

Figure 8. CV curves of **HBPO-Fc1** film (A) and **HBPO-Fc2** film (B) in water with successive 20 cycles. Electrolyte: 0.1 M $LiClO_4$. [Fe]: 1.0 μmol/cm^2. Scan rate: 0.1 V/s.

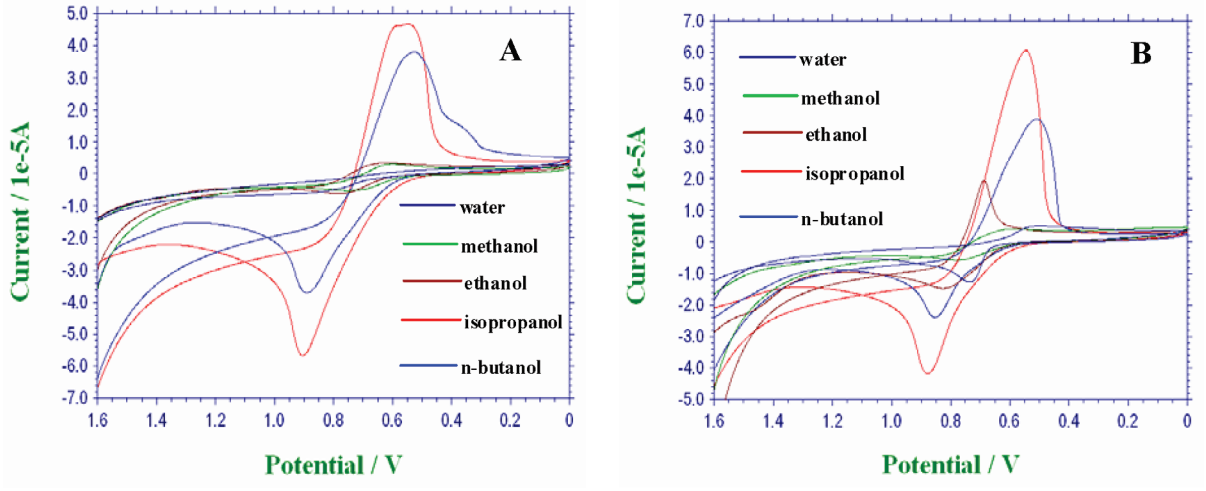

Figure 9. CV curves of **HBPO-Fc1** film (A) and **HBPO-Fc2** (B) in varous solvents. Electrolyte: 0.1 M $LiClO_4$. [Fe]: 1.0 μmol /cm^2. Scan rate: 0.1 V/s.

Table 4. Quantity of Electricity in the Reduction and Oxidation Processes of HBPO-Fc1 and HBPO-Fc2

	Q_C (10^{-6} C)			
	HBPO-Fc1		**HBPO-Fc2**	
solvents	reduction peak	oxidation peak	reduction peak	oxidation peak
water			5.329	5.661
methanol	5.656	4.991	10.03	5.828
ethanol	7.994	5.550	15.48	16.10
2-propanol	75.34	34.00	75.86	29.60
n-butanol	48.83	25.35	46.40	46.40

and **HBPO-Fc2** to different anions such as $H_2PO_4^-$, HSO_4^-, and Br^-. It was found that with the addition of anions, CV curves of **HBPO-Fc1** and **HBPO-Fc2** changed apparently. The peak potential changed little, but the peak currents changed a lot. With the increase of anion amounts, the peak currents decreased. When anion amount reached a higher value, the CV curves became unstable. The responses of **HBPO-Fc1** and **HBPO-Fc2** to anions were different with other ferrocenyl anion receptors,[5−7] and this may be caused by two reasons, one of which was that the hyperbranched polymer **HBPO-Fc1** and **HBPO-Fc2** adsorbed on the electrode in a serious manner. The other reason may be that the binding sites of **HBPO-Fc1** and **HBPO-Fc2** were ester group and hydroxyl group, which just bound anions with weak interactions. The anion binding of **HBPO-Fc1** and **HBPO-Fc2** influenced the surface exchange efficiency and mass diffusion and thus influenced the CV curves of **HBPO-Fc1** and **HBPO-Fc2**.

From the change of peak currents of **HBPO-Fc1** and **HBPO-Fc2**, we can also obtain their anion binding capability. Figure 11 showed the changes of reduction peak currents of **HBPO-Fc1** and **HBPO-Fc2** with the amounts of anions. It was found that with the increase of $H_2PO_4^-$, the peak currents of **HBPO-Fc1** decreased rapidly. For HSO_4^-, the decrease rate of peak currents was smaller than that of $H_2PO_4^-$. And Br^- caused the smallest decrease rate of peak currents of **HBPO-Fc1**. The order of the peak current decreasing rate indicated the anion binding capacity order of **HBPO-Fc1**, which was $H_2PO_4^- > HSO_4^- > Br^-$. **HBPO-Fc2** showed largest binding capacity of $H_2PO_4^-$ as well, but showed smaller binding capacity of HSO_4^- than Br^-. Due to

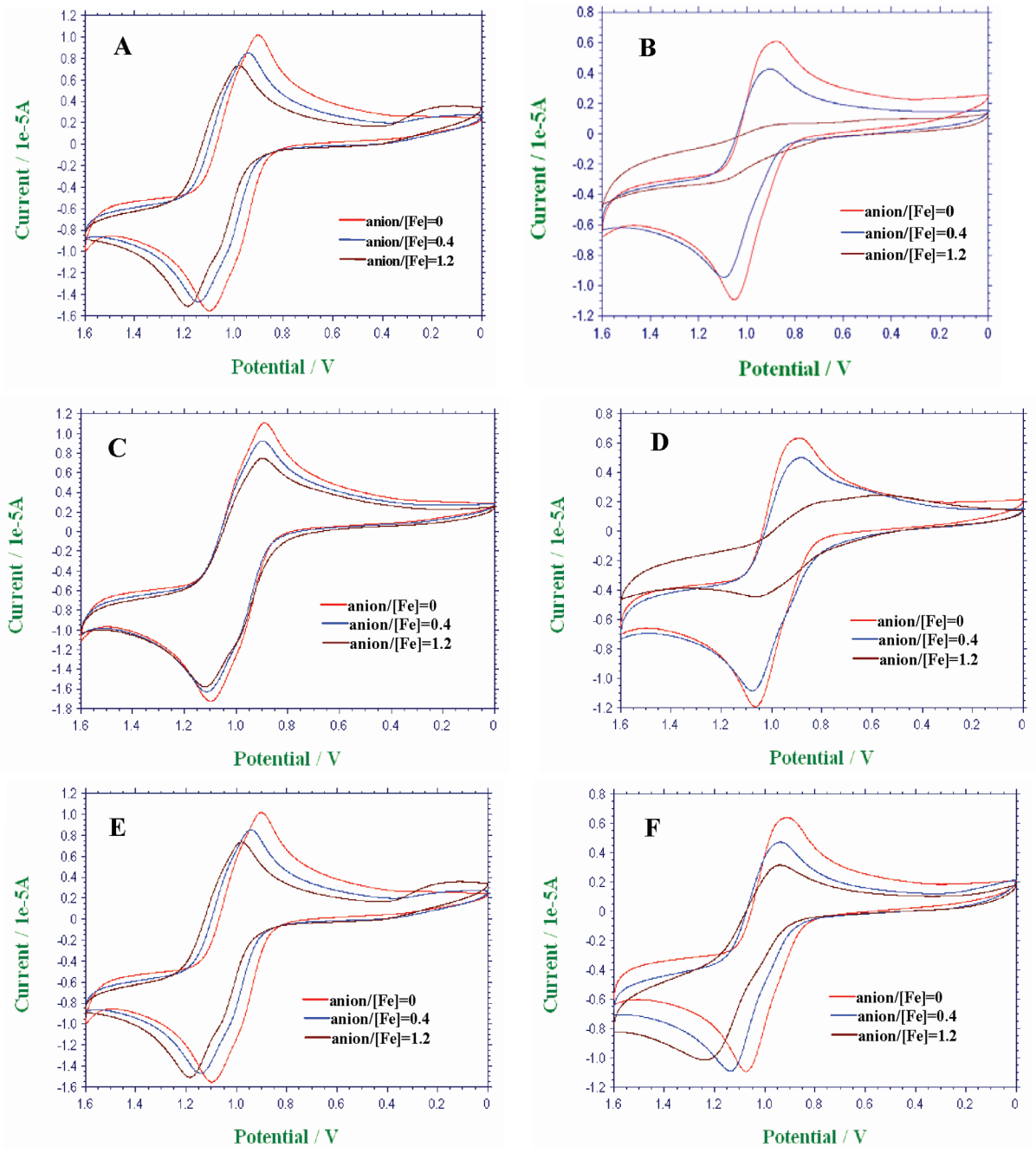

Figure 10. CV curves of **HBPO-Fc1** and **HBPO-Fc2** after addition of $H_2PO_4^-$, HSO_4^- and Br^- in CH_2Cl_2: (A) **HBPO-Fc1**with $H_2PO_4^-$; (B)**HBPO-Fc2** with $H_2PO_4^-$; (C) **HBPO-Fc1** with HSO_4^-; (D) **HBPO-Fc2** with HSO_4^-; (E) **HBPO-Fc1**with Br^-; (F) **HBPO-Fc2** with Br^-.

the different initial peak currents, the comparison of anion binding capacity of **HBPO-Fc1** and **HBPO-Fc2** through the decrease of peak current seemed unavailable. However, instead the peak current i_{pc} of i_{pc}/i_{pc}^0, in which i_{pc}^0 was initial peak current of **HBPO-Fc1** and **HBPO-Fc2** without any anion added, investigation of the change of i_{pc}/i_{pc}^0 with the anion amounts would be meaningful. Figure 12 showed the changes of i_{pc}/i_{pc}^0 with anion amounts. It was found that for the three anions, $H_2PO_4^-$, HSO_4^-, and Br^-, **HBPO-Fc2** showed a much larger i_{pc}/i_{pc}^0 decrease rate than **HBPO-Fc1** and thus a much larger binding capacity.

3.3.2. Anion Recognition Investigation of HBPO-Fc by UV−vis. UV−vis was used to investigate the anion recognition of **HBPO-Fc1** and **HBPO-Fc2** (Figure 13). It was found that when anions were added, the intensities of the peaks at 322 and 256 nm decreased, indicating the binding of anions by **HBPO-Fc1** and **HBPO-Fc2**. The insets showed the changes of intensity at 322 nm with the amounts of anions. We find that the intensity at 322 nm of **HBPO-Fc1** showed step changes. For **HBPO-Fc1**, when $H_2PO_4^-$ was added, the intensity decreased dramatically. However, when the amount of $H_2PO_4^-$ reached 1 equiv of the ferrocene group, the intensity stopped changing. As for HSO_4^- and Br^-, the phenomena were similar to $H_2PO_4^-$. After the amount of HSO_4^- or Br^- reached to one equivalent, the intensity decrease rate suddenly lowered. Thus, from the step change of the intensity of **HBPO-Fc1**, the binding model of **HBPO-Fc1** to $H_2PO_4^-$, HSO_4^-, and Br^- can be given that **HBPO-Fc1** bound these anions with binding model of 1:1. As for **HBPO-Fc2**, the step change phenomena of intensity at 322 nm were different with **HBPO-Fc1**. When $H_2PO_4^-$ or HSO_4^- were added, the intensity at 322 nm slightly

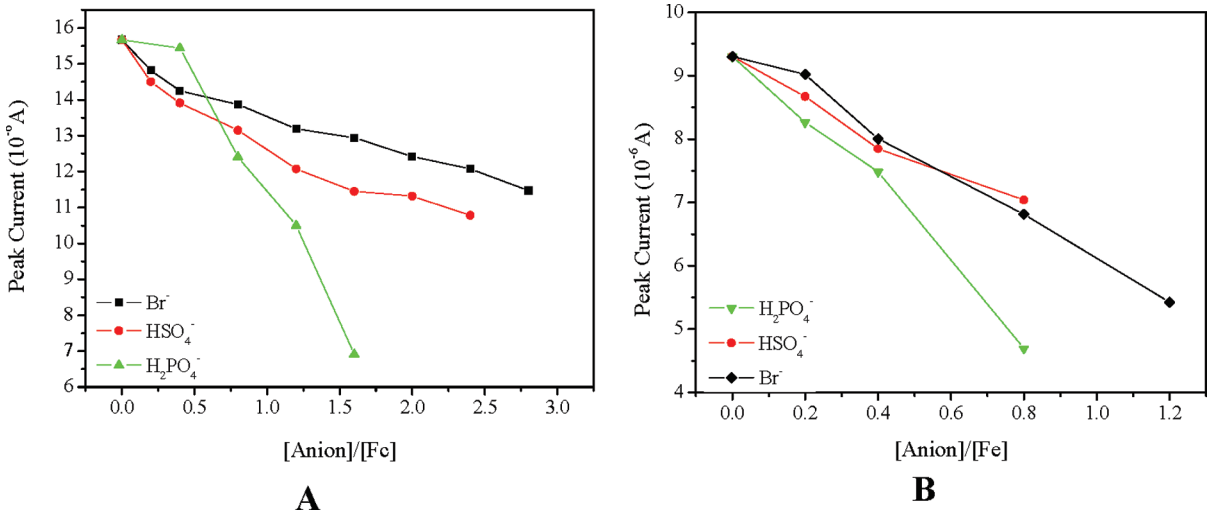

Figure 11. Changes of the reduction peak currents of **HBPO-Fc1** (A) and **HBPO-Fc2** (B).

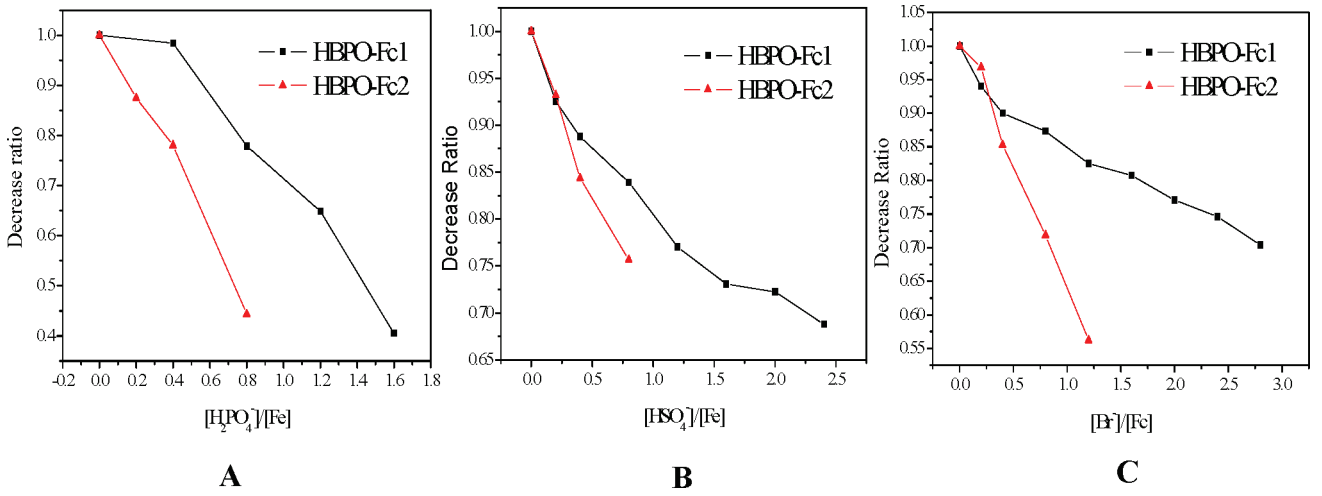

Figure 12. Comparison of **HBPO-F1** and **HBPO-Fc2** in the recognition of $H_2PO_4^-$ (A), HSO_4^- (B), and Br^- (C).

decreased. When the amount of $H_2PO_4^-$ or HSO_4^- reached 0.5 equiv of the ferrocene group, the intensity decrease rate suddenly became greater. Then when amounts of $H_2PO_4^-$ or HSO_4^- reached to 1.0 equivalent of ferrocene group, the decrease rate of intensity again lowered. For Br^-, the step change phenomena of intensity at 322 nm seemed unclear, but the intensity change at 256 nm was apparent, and clearly showed the key point of 0.5 equiv. Thus the binding model of **HBPO-Fc2** to anions was different with **HBPO-Fc1**. The binding process of **HBPO-Fc2** to anions may involve the transformation of the 1:2 model to the 1:1 model.

The different anion binding models of **HBPO-Fc1** and **HBPO-Fc2** were determined by their different structures. For **HBPO-Fc1**, the carbonyl group and ferrocene group were relatively smaller, and the hydroxyl group content was relatively larger, thus it can bind anions with the synergy of carbonyl group and hydroxyl group with 1:1 mode as shown in Figure 14A. But for **HBPO-Fc2**, the carbonyl group and ferrocene group were relatively larger, thus it mainly rely on carbonyl group to bind anions. When anions were added, **HBPO-Fc2** first bound anions by the synergy of two carbonyl groups with the mode of 1:2 mode just as shown in Figure 14B. When anion amount further increased, **HBPO-Fc2** changed the binding mode to 1:1 mode with just one carbonyl group as shown in Figure 14C.

4. Conclusion

In conclusion, electrochemical behavior and anion recognition of a kind of novel ferrocenyl hyperbranched ether **HBPO-Fc** were studied. Influence of ferrocene content, scan rate, solvents and electrolyte concentration on electrochemical behaviors were investigated, and it was found that with more ferrocene content, **HBPO-Fc2** showed lower peak currents because of the different redox center density. And with increasing scan rate, the reduction peak shifted to lower potential, and the oxidation peak shifted to the higher potential, and the peak currents also increased. From the relationship of peak potential, peak current and scan rate, dynamic parameters of the electrode process were obtained. In different solvents, **HBPO-Fc** showed different electrochemical behaviors, and in polar solvents such as DMF and DMSO, the CV curves were badly distorted, but in moderate polar solvents such as CH_2Cl_2 and $CHCl_3$, the CV curves showed high symmetric peak shapes. With the increase of electrolyte concentration, the peak-to-peak potential separation increased, and when in lower electrolyte concentration, the peak-to-peak potential separation changed dramatically, but when in high electrolyte concentration, the influence of electrolyte concentration seemed unclear. The electrode dynamic parameter in different solvents and different electrolyte concentration were also obtained.

Anion recognition of **HBPO-Fc** was investigated in CH_2Cl_2. And when $H_2PO_4^-$, HSO_4^-, or Br^- was added, the peak currents

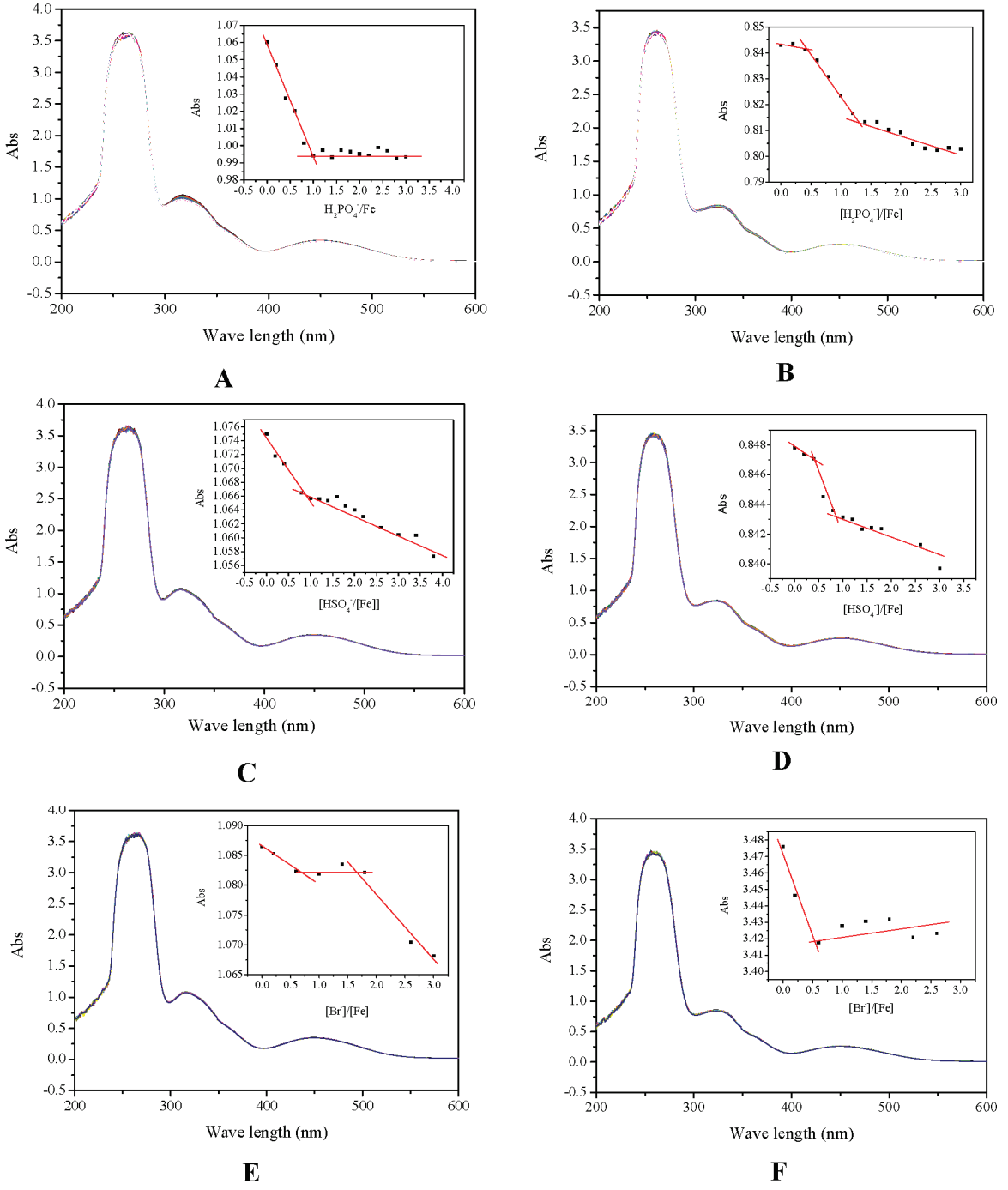

Figure 13. UV−vis spectra of **HBPO-Fc1** and **HBPO-Fc2** upon addition with the different anions; (A) **HBPO-Fc1** with $H_2PO_4^-$, (B) **HBPO-Fc2** with $H_2PO_4^-$, (C) **HBPO-Fc1** with HSO_4^-, (D) **HBPO-Fc2** with HSO_4^-, (E) **HBPO-Fc1** with Br^-, and (F) **HBPO-Fc2** with Br^-. The insets are changes of the intensity of peak at 322 nm with anions amounts for parts A−E, and for part F, the inset is the intensity of the peak at 256 nm with anion amount.

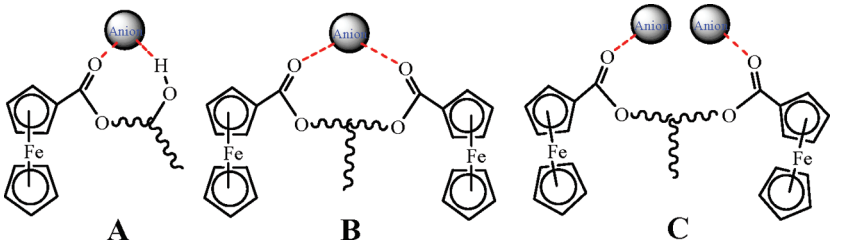

Figure 14. Possible binding modes of **HBPO-Fc1** and **HBPO-Fc2**.

of **HBPO-Fc** decreased dramatically. And through the peak currents decrease rate, the anion binding capacity can be obtained. $H_2PO_4^-$ led to the fastest peak currents decrease rate of **HBPO-Fc1**, and then the HSO_4^-, Br^- caused the slowest,

which indicated the anion binding capacity order of **HBPO-Fc1**: $H_2PO_4^-$ > HSO_4^- > Br^-. For **HBPO-Fc2** with higher ferrocene content, the anion binding capacity order was: $H_2PO_4^-$ > Br^- > HSO_4^-. UV−vis was used to investigate the anion recognition of **HBPO-Fc**. When $H_2PO_4^-$, HSO_4^- or Br^- was added, the intensity of the peak at 322 and 256 nm of **HBPO-Fc1** and **HBPO-Fc2** decreased. For **HBPO-Fc1**, the dramatic decrease of the intensity at 322 nm suddenly lowered when amount of $H_2PO_4^-$, HSO_4^-, or Br^- reached 1 equiv of the ferrocene group. As for **HBPO-Fc2**, the decrease of the intensity at 322 nm were slow when the amounts of $H_2PO_4^-$, HSO_4^-, or Br^- were small, but when their amount reached 0.5 equiv of the ferrocene group, the intensity decrease at 322 nm suddenly became dramatic, and when the amount reached a higher value, 1.0 equiv, the intensity decrease at 322 nm gradually lowered again. The step change of the intensity at 322 nm of **HBPO-Fc1** and **HBPO-Fc2** indicated the different binding models of these moieties to anions.

Acknowledgment. This work is supported by the National Nature Science Foundation of China (No. 20672097 and No.20772108) and Science and Technology Program of Ningbo. We also thank Prof. R. James Cross, Yale University, for kind discussions.

Supporting Information Available: Table showing the linear relationship among peak currents, peak potential, and scan rate. This material is available free of charge via the Internet at http://pubs.acs.org.

References and Notes

(1) Beer, P. D.; Hayes, E. J. *Coord. Chem. Rev.* **2003**, *240*, 67.
(2) Beer, P. D.; Gale, P. A. *Angew.Chem., Int. Ed.* **2001**, *40*, 486.
(3) Reynes, O.; Bucher, C.; Moutet, J. C.; Royal, G.; Aman, E. S.; Ungureau, E. M. *J. Electroanal. Chem.* **2005**, *580*, 291.
(4) Valério, C.; Fillaut, J. L.; Ruiz, J.; Guittard, J.; Blais, J. C.; Astruc, D. *J. Am. Chem. Soc.* **1997**, *119*, 2588.
(5) Astruc, D.; Daniel, M. C.; Ruiz, J. *Chem. Commun.* **2004**, 2637.
(6) Daniel, M. C.; Ruiz, J.; Blais, J. C.; Daro, N.; Astruc, D. *Chem.—Eur. J.* **2003**, *9*, 4371.
(7) Ruiz, J.; Jesus, M.; Medel, R.; Daniel, Ma. C.; Blais, J. C.; Astruc, D. *Chem. Commun.* **2003**, 464.
(8) Tan, H. M.; Luo, Y. J. *Hyperbranched Polymers*; Chemical Industry Press: Beijing, 2005.
(9) (a) Shi, J. B.; Tong, B.; Li, Z.; Shen, J. B.; Zhao, W.; Fu, H. H.; Zhi, J. G.; Dong, Y. P.; Hussler, M.; Lam, J. W. Y.; Tang, B. Z. *Macromolecules* **2007**, *40*, 8195. (b) Shi, J. B.; Tong, B.; Zhao, W.; Shen, J. B.; Zhi, J.; Dong, Y. P.; Hussler, M.; Lam, J. W. Y.; Tang, B. Z. *Macromolecules*. **2007**, *40*, 5612. (c) Li, Z.; Lam, J. W. Y.; Dong, Y. Q.; Dong, Y. P.; Sung, H. H. Y.; Williams, I. D.; Tang, B. Z. *Macromolecules* **2006**, *39*, 6458. (d) Sun, Q. H.; Xu, K. T.; Peng, H.; Zheng, R. H.; Hussler, M.; Tang, B. Z. *Macromolecules* **2003**, *36*, 2309.
(10) Deng, L. B.; Wang, L.; Yu, H. J.; Wang, J. J.; Dong, X. C. *J. Appl. Polym. Sci.* **2008**, *107*, 1539.
(11) Wang, X. J.; Wang, L.; Wang, J. J.; Chen, T. *J. Phys. Chem. B* **2004**, *108*, 5627.
(12) Chen, T.; Wang, L.; Jiang, G. H.; Wang, J. J.; Dong, X. C.; Wang, X. J.; Zhou, J. F.; Wang, W.; Wang, C. L. *J. Phys. Chem. B* **2005**, *109*, 4624.
(13) Chen, T.; Wang, L.; Jiang, G. H.; Wang, J. J.; Wang, X. J.; Zhou, J. F.; Wang, J. F.; Chen, C.; Wang, W. *J. Electroanal. Chem.* **2006**, *586*, 122.
(14) Huo, J.; Wang, L.; Yu, H. J.; Deng, L. B.; Zhou, J. F.; Yang, Q. *J. Polym. Sci: B* **2007**, *45*, 2880.
(15) Pattison, D. B. *J. Am. Chem. Soc.* **1957**, *79*, 3455.
(16) Yan, D. Y.; Hou, J.; Zhu, X. Y.; Kosman, J. J.; Wu., H. S. *Macrom. Rap. Comm.* **2000**, *21*, 557.
(17) Jiang, G. H.; Wang, L.; Chen, T.; Yu, H. J.; Wang, C. L.; Chen, C. *Polymer*. **2005**, *46*, 5351.
(18) Bard, A. J.; Faulkner, L. R. *Electrochemical Methods*; John Wiley & Sons Inc.: New York, 1980.
(19) Heo, R. W.; Park, J.; Lee, T. R. *Macromolecules* **2005**, *38*, 2564.
(20) Wu, S.; Chen, Y.; Zeng, F.; Gong, S.; Tong, Z. *Macromolecules* **2006**, *39*, 6796.